Effect Mechanism of Ice Crystals on Mechanical Properties of Shale Ceramsite Concrete

Qinting Wang[1, 2], Yuhang Qiu[2], Jianqing Zhao[1], Jianhui Yang[1, 2, *] and Dejun Liu[3]

[1]*International Joint Research Laboratory of Henan Province for Underground Space Development and Disaster Prevention, Henan Polytechnic University, Jiaozuo 454003, China*
[2]*Henan Province Engineering Laboratory for Eco-architecture and the Built Environment, Henan Polytechnic University, Jiaozuo 454000, China*
[3]*School of Civil Engineering and Architecture, Jiaxing University, Jiaxing 314001, China*

_____

Abstract

To investigate the mechanism responsible for the embrittlement of concretes containing lightweight aggregates at cryogenic temperatures, a series of experiments were performed on all-lightweight shale ceramsite concrete (ALWSCC) and icicles at temperatures from -5 to -15 °C. The mechanical properties of ALWSCC specimens at cryogenic temperatures were analysed, the dependence of cryogenic mechanical properties on ice crystal volume and freezing temperature was also investigated. The Hansen model was used to invert the elastic modulus of ice crystals by a step-by-step approach. Results show that the compressive strength of ALWSCC specimens increases with the increasing volume fraction of ice crystals, and the strengthening effect gradually decreases after the ice crystal volume fraction exceeds 16.5%. The cubic compressive strength of ALWSCC specimens with ice crystals is more sensitive to freezing temperatures than that of dried ALWSCC specimens. Shear failure occurs when icicles are compressed, and the density and strength of ice increase with decreasing temperature below the freezing point. The elastic modulus of ice crystals is much higher than that of icicles at the same temperature, showing a huge size effect, and the ratio of the elastic modulus is less affected by temperature. The conclusions obtained in this study are important for understanding the mechanism of variation in the material properties of lightweight aggregate concrete in regions that experience cryogenic temperatures.

Keywords: Shale ceramsite concrete, Ice crystal, Elastic modulus, Hansen model

_____

1. Introduction

Shale ceramsites are high-quality lightweight aggregates that can be mixed with shale pottery sand to prepare all-lightweight shale ceramsite concrete (ALWSCC). The apparent density of ALWSCC is only 1950 kg/m³, and ALWSCC has good thermal insulation properties. In addition, it is easy to prepare structural ALWSCC of LC30 grade from cement, shale ceramsites, shale pottery sand, fly ash and water. Therefore, ALWSCC is a relatively ideal energy-saving material for buildings in cold regions [1-2]. ALWSCC is a multiphase composite material composed of solid, gaseous and liquid substances and its physicochemical properties undergo a series of continuous changes at cryogenic temperatures [3]. Consequently, the strength and elasticity modulus of ALWSCC change significantly at cryogenic temperatures compared to room environments, especially in cold regions such as North America, Northern Europe and Northern China.

The strength and elastic modulus of concrete containing ordinary aggregate increase as the temperature decreases, but the strain corresponding to the peak stress decreases, indicating that concrete at cryogenic temperatures is significantly more brittle [4]. Temperature and moisture content are important factors affecting the strength enhancement of cryogenic concrete [5]. In cryogenic environments, the water inside the concrete condenses into ice crystals that fill the pores, increasing the overall density and reducing the concentrated stress in the concrete during compression [6]. High porosity gives light aggregate concrete more space to store ice, and the mechanical behaviour of light aggregate concrete is more affected by ice crystals in cold regions. The mechanical response of lightweight concrete at cryogenic temperatures is the result of the synergistic action of ice crystals and the matrix when considered from the perspective of composite materials [7].

However, these results above mentioned are mostly devoted to the macroscopic mechanical properties and freeze-thaw damage of concrete, while the mechanism by which ice crystals affect the mechanical properties of concrete is not clear. The mechanical properties of concrete under cryogenic conditions are the basis for the design of buildings and structures in cold regions. The study of the mechanism of the effects of ice crystals on the mechanical properties of lightweight aggregate concrete is of great significance for the engineering application of ALWSCC under cryogenic conditions.

2. State of the art

At negative temperatures, the strength and elastic modulus of concrete increase, exhibiting significant temperature sensitivity. Jiang et al. characterized the thermodynamic freezing process and pore size distribution of water in mortar using differential scanning calorimetry (DSC) and thermal

_____

profilometry (TPM). They found that the water content and initial strength of mortar at room temperature are the main factors affecting its strength at cryogenic temperatures, and that ice formation in capillary pores and gel pores is intrinsically responsible [8]. Wang et al. concluded that ice crystals have two effects on concrete: (*a*) ice crystals enhance the overall performance of water because they are harder than liquid water in pores; and (*b*) excessive amounts of ice crystals can exert high pressure on the pore walls, weakening the overall ability of the material to resist damage. The increase or decrease in concrete strength at cryogenic temperatures depends on whether effect (*a*) or effect (*b*) is dominant [9]. After reviewing the mechanical properties of concrete at cryogenic temperatures, Jiang et al. also concluded that temperature and moisture content are the main factors affecting the strength variation of concrete and obtained the maximum compressive strength of concrete at a temperature of -120°C through tests [10]. For quantitative characterization, Masad et al. used finite element analysis to calculate the mechanical parameters of concrete at cryogenic temperatures and analysed the effects of aggregate particle properties (size, thermal expansion coefficient, volume fraction and shape) on damage to concrete at cryogenic temperatures. The results indicate that the difference in the thermal expansion coefficients of mortar and aggregate is an important factor affecting the development of damage. The coefficient of thermal expansion of lightweight aggregates is smaller than that of ordinary aggregates, and there is a need to investigate the mechanical properties of lightweight aggregates in the cryogenic state [11-13].

Lightweight aggregates are porous, resulting in a significant reduction in the overall concrete density. In a wet environment, concrete that contains light aggregate stores large amounts of water that forms ice crystals at negative temperatures, which impacts the overall performance of the concrete. Kogbara et al. prepared four types of concrete with different coarse aggregates, limestone, sandstone, igneous rock and light aggregate, for test at cryogenic temperatures, used an acoustic emission metre to observe the microcrack expansion process during the freezing of concrete cubes, and found that lightweight aggregate concrete was stronger (more resistant to damage at cryogenic temperatures) than normal aggregate concrete [14]. Liu et al. prepared a new ultralightweight cement composite and experimentally investigated its mechanical properties at -60°C. The results showed that the compressive strength of ordinary concrete and lightweight concrete generally increased with decreasing temperature [15]. However, the same phenomenon was not observed in an ultralight cement composite. The available studies of the mechanical properties of lightweight concrete at cryogenic temperatures are limited, the results in the literatures [15] and [16] show that the cryogenic mechanical properties of lightweight aggregate concrete vary considerably with the aggregate, and the mechanism responsible for the effects of ice crystals on the mechanical properties of lightweight aggregate concrete deserves in-depth study.

In summary, the temperature, ice crystal volume and thermal expansion coefficients of aggregates are the main reasons for the different mechanical properties of concrete at cryogenic temperatures, and the larger amounts of space to store ice and smaller thermal expansion coefficients of light aggregates, compared with those of ordinary aggregates, affect the overall properties of concrete in cryogenic environments [17-19]. However, research on lightweight aggregate concrete at cryogenic temperatures is not sufficient, and the mechanism of ice crystal enhancement has not been revealed [20-22]. Therefore, this paper researched LC30 grade ALWSCC and investigated the dependence of cryogenic mechanical properties on ice crystal volume and freezing temperature. Next, the physical and mechanical properties of icicles were tested to understand the rules describing the changes in density, elastic modulus and strength. Finally, a composite mechanics method was used to invert the elastic modulus of ice crystals and reveal the mechanism for the influence of ice crystals on the mechanical properties of lightweight aggregate concrete. This study provided a theoretical basis and parametric guidance for the application of lightweight concrete in cold regions

The rest of this study is organized as follows. Section 3 describes the material and the experimental methods. Section 4 gives the results and discussion, and finally, the conclusions are summarized in Section 5.

3. Methodology

3.1 Material and mix proportion

Icicles were prepared by freezing tap water at cryogenic temperatures. The raw materials for ALWSCC consisted of cement, fly ash, shale ceramsite, shale pottery sand, water reducing agent and water. The cement was ordinary P.O. 42.5 grade silicate cement, and met the requirements of ASTM type I, as shown in Table 1. The fly ash met the requirements of ASTM class B, with a density of 2347.15 kg/m^3, and the fly ash was 25% of the mass of the cementitious material. The maximum particle size of the shale ceramsite was 15 mm, the bulk density was 620 kg/m^3, the tube crushing strength was 3.7 MPa, and the 24 h water absorption was 9.6%. The maximum particle size of shale pottery was 5 mm, the bulk density was 880 kg/m^3, the 24 h water absorption was 12.5%, and the fineness modulus was 2.5. The water reducing agent was from the naphthalene series, and it was used at 2.0% of the cementitious material. As shown in Table 2, the composition of ALWSCC with a strength grade of 30 MPa was determined by orthogonal tests.

3.2 Specimen preparation

ALWSCC was prepared according to Table 2, and the shale ceramsite was wetted for 24 h before mixing. The newly mixed ALWSCC was demoulded after 1 d, then cured for 28 d under standard conditions (relative humidity not less than 95% and room temperature at 20 °C). A cubic specimen of size 100 mm × 100 mm × 100 mm was used for the compressive strength test (Fig. 1(a)), and a prismatic specimen of size 100 mm × 100 mm × 300 mm was used for the elastic modulus and stress-strain curve tests. To prepare specimens with different ice crystal volume fractions, the water absorption characteristics of ALWSCC were determined. The cubic specimens were placed in water and weighed at different time intervals. The water content was defined as the ratio of the mass of water to the mass of the cubic specimen, and its value varied with time, as shown in Fig. 2. Using the immersion method, ALWSCC samples with water contents of 3.48%, 6.3%, 8.97%, 10.57%, 10.87%, 11.05%, and 11.06% were made and frozen in cryostats at target temperatures of -5°C, -10°C, and -15°C for 3 d to prepare ALWSCC specimens with different ice crystal volume fractions. The formula for calculating the volume fraction of ice crystals is shown in Eq. (1).

$$V_i = \frac{m_c \times w}{V_c \times \rho_i} \times 100\% \tag{1}$$

where V_i (%) is the volume fraction of ice crystals. m_c (kg) and V_c (m³) are the mass and volume of concrete, respectively. w is the water content and ρ_i (kg/m³) is the density of ice crystals.

Table. 1. Physical and mechanical properties of cement.

Strength grade	Specific surface area (m²/kg)	Fineness (%)	Loss on ignition (%)	SO₃ (%)	MgO (%)	Initial/Final setting time (min)	f_{cu} (MPa)	f_{bs} (MPa)
42.5	400	1.3	2.41	2.45	2.11	210/265	29.5	8.5
Notes	f_{cu} is the cubic compressive strength after standard curing for 28 d, f_{bs} is the cubic flexural strength after standard curing for 28 days.							

Table. 2. Composition of ALWSCC (kg/m³).

Group	Cement	Fly ash	Shale ceramsite	Shale sand	Water	Water reducing agent	Dry apparent density
ALWSCC	458.10	149.52	422.86	388.57	162.86	12.15	1477.78

Icicle specimens were made by freezing water in a cryostat using a stainless-steel mould of Φ 50 mm × 100 mm. The detailed steps can be expressed as follows: (*a*) tap water was poured into the mould and put into the DW-40 cryostat at -5°C for 3 h; (*b*) icicles were demoulded, and their two end surfaces were smoothed and wrapped with cling film to form semi-finished specimens; and (*c*) semi-finished specimens were placed into the cryostat at -5°C, -10°C and -15°C for 3 d, as shown in Fig. 1(b).
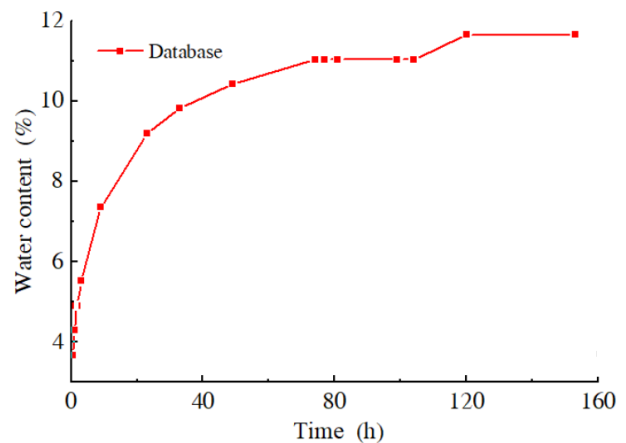

(a) Cubic specimens

(b) Icicle specimens
Fig. 1. Some specimens for testing.

Fig. 2. Relationship between the moisture content of ALWSCC and the immersion time in water.

3.3 Test Method
ALWSCC and icicles underwent uniaxial compressive strength tests and elastic modulus tests that were performed with an SYE-2000 electrohydraulic servo universal material testing machine, as shown in Fig. 3. Groups of five specimens were loaded at a rate of 0.5 MPa/s. The strength test of ALWSC was carried out using nonstandard cubic specimens with a size of 100 mm × 100 mm × 100 mm, and the results were multiplied by a conversion factor of 0.95 (GB/T 50081-2019 in China). To reduce the impact of the external environment, the specimens were tested immediately after removal from the cryostat. When icicles were tested, a large stiff composite plate was used to insulate the upper and lower dies in the test machine (Fig. 3(b)).

4. Results and Discussion

4.1 The effect of the ice crystal volume fraction on the strength of ALWSCC
The effect of the ice crystal volume fraction on the compressive strength of ALWSCC specimens is shown in Fig. 4, and least squares fitting was used to obtain the relationship expressed by Eq. (2). At -10°C, the compressive strength of ALWSCC increased with increasing ice crystal volume fraction.
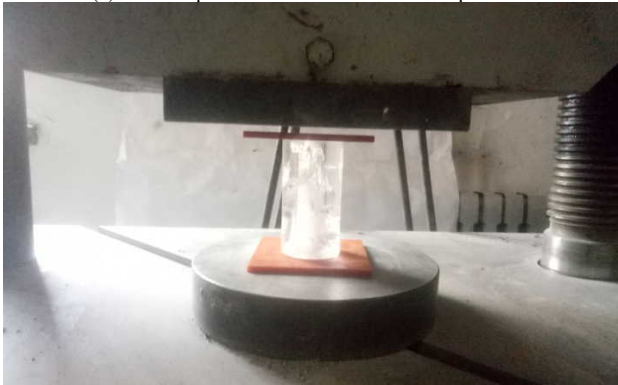
$$f_{cu}' = -0.0027V_i + 0.1359V_i + 32.2647 \quad R^2 = 0.9890 \tag{2}$$

where f'_{cu} (MPa) is the compressive strength of ALWSCC at a cryogenic temperature.

(a) The compression test of an ALWSCC specimen

(b) The compression test of an icicle
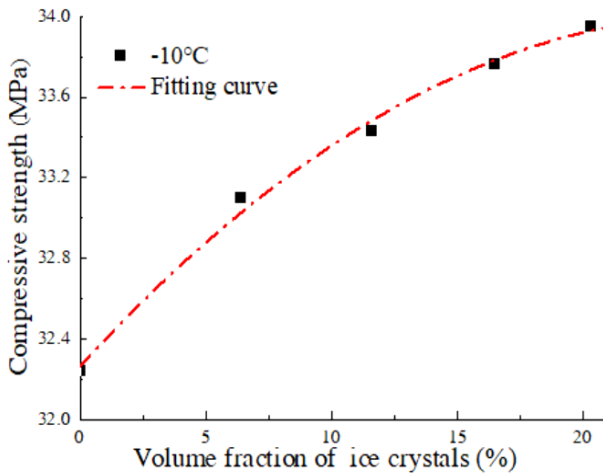
Fig. 3. Test equipment and method.

Fig. 4. Relationship between the cubic specimen compressive strength and ice crystal volume fraction (at -10°C).

Compared with the dried ALWSCC specimens, the compressive strength of ALWSCC specimens with ice crystal volume fractions of 6.4%, 11.6%, 16.5% and 20.34% increased by 1.5%, 3.2%, 4.5% and 5.3%, respectively. After the volume fraction of ice crystals exceeded 16.5%, the enhancement effect of ice crystals on the ALWSCC matrix gradually decreased. Under negative temperature conditions, the liquid water in ALWSCC froze into ice crystals that filled the pores in the cement matrix and aggregate. According to the theory of composite mechanics, both the cement matrix and aggregates were strengthened by ice crystals, causing an increase in the overall strength of ALWSCC.

4.2 The effect of freezing temperature on the mechanical properties of ALWSCC

As shown in Fig. 5(a), the mechanical properties of ALWSCC with a 20% volume fraction of ice crystals were tested after freezing at different cryogenic temperatures, and dried concrete was used as a reference. Both the compressive strength and elastic modulus of ALWSCC specimens gradually increased with decreasing freezing temperature, and the compressive strength of ALWSCC specimens containing ice crystals (20% volume fraction) was more sensitive than dried ALWSCC to the freezing temperature. At room temperature, the strength of the ALWSCC specimens that contained water decreased by 4.62% compared to the dried state. When the temperature was lowered below -15°C, the strength of the ALWSCC specimens containing a 20% volume fraction of ice crystals was enhanced by 7.27% compared to the dried state. When the temperature was lower, the enhancement effect of ice crystals on ALWSCC was more significant.

The ratio of the compressive strength of the ALWSCC specimens at cryogenic temperatures to that at room temperature is shown in Fig. 5(b), and the equation fitting compressive strength vs temperature is shown in Eq. (3). The ratio gradually increases with decreasing temperature.
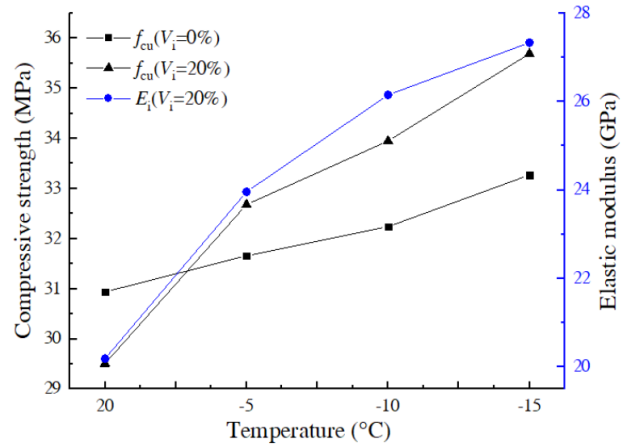
(a) Compressive strength and elastic modulus
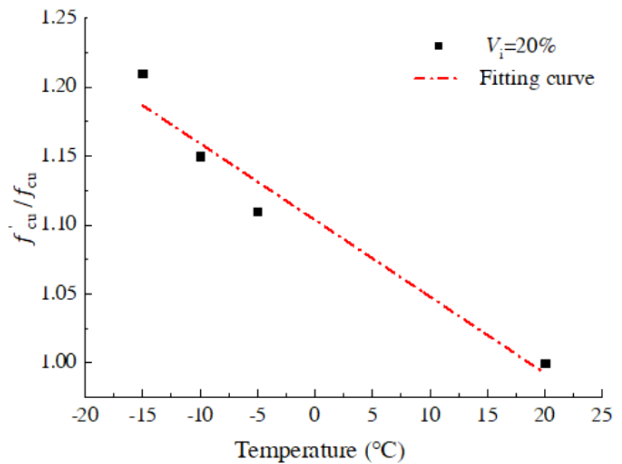
(b) Ratio of compressive strength

Fig. 5. Mechanical properties of the ALWSCC specimens after cryogenic freezing.

$$\frac{f'_{cu}}{f_{cu}} = -0.006T + 1.1 \qquad V_i = 20\% \qquad R^2 = 0.9899 \qquad (3)$$

4.3 Physical and mechanical properties of icicles

The relationships describing the variation of ice density with freezing time are shown in Fig. 6, and the trend can be divided into three stages: (*a*) from 0 h to 24 h at cryogenic temperatures, the density decreased linearly with time, and the freezing phenomenon gradually extended from the outermost layer to the interior of the water, accompanied by the formation of strip-shaped bubbles and large bubbles; (*b*) from 24 h to 72 h at cryogenic temperatures, the density increased nonlinearly with time, and the water completely froze into ice, accompanied by the gradual disappearance of the bar-shaped bubbles and large bubbles from inside the ice column; and (*c*) after 72 h at cryogenic temperatures, the density of ice remained almost constant, and the relationship between density and temperature was obtained in Eq. (4).
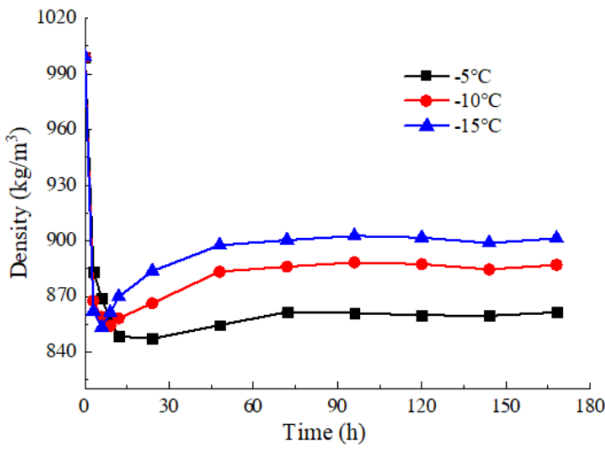

Fig. 7. Damage pattern of icicles.

Fig. 6. The relationship between the density of icicles and the time at different cryogenic temperatures.
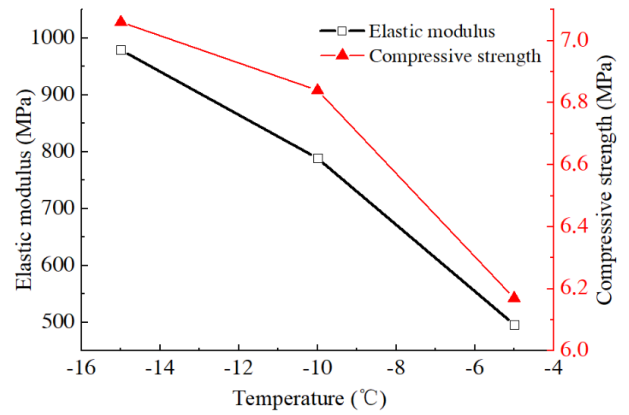
$$\rho_i = -3.88T + 843.86 \qquad R^2 = 0.954 \qquad (4)$$

The icicles were tested for compressive strength after freezing at the target temperatures for 3 d. During compression, the icicles exhibited typical brittle material properties. At the initial phase of the test, there was no significant change in the specimens. When icicles were loaded near their peak stress, the surface layer began to peel off each icicle. Shortly thereafter, with a crisp sound, each specimen was destroyed. The dominant failure modes were shear failure with a splitting surface angle of approximately 63°, as shown in Fig. 7.
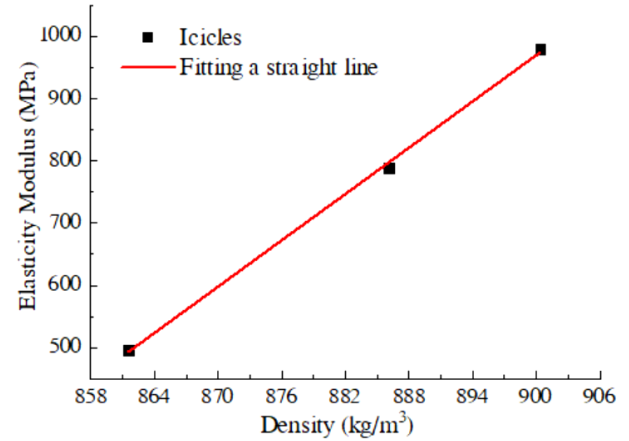
The elastic modulus and uniaxial compressive strength of the icicles gradually increased with decreasing temperature, as shown in Fig. 8(a). At -5°C, the uniaxial compressive strength and elastic modulus of the icicles were 6.17 MPa and 496.28 MPa, respectively, which were less strong and stiff than the concrete material. However, the strength and stiffness of the icicles increased rapidly with decreasing temperature. At -10°C and -15°C, the strength of the icicles increased by 10.86% and 14.42%, and the elastic modulus increased by 58.92% and 97.31%, respectively. When the temperature was lower, the internal structure of the icicles was denser, causing an increase in strength and elastic modulus. The variation of the elastic modulus of the icicles with density is shown in Fig. 8(b), and the linear relationship between the two variables is obtained by fitting, as shown in Eq. (5).

(a) Elastic modulus and compressive strength

(b) Elasticity modulus

Fig. 8. Compressive strength and elastic modulus of icicle.

$$E_i = 12.39\rho_i - 10182.97 \qquad R^2 = 0.99815 \qquad (5)$$

where E_i (MPa) is the elastic modulus of the icicle.

4.4 Mechanism of the effects of ice crystals on the mechanical properties of ALWSCC

At cryogenic temperatures, ALWSCC specimens that contain ice can be considered a two-phase composite consisting of a matrix and ice crystals, as shown in Fig. 9(a). The dried ALWSCC is considered a two-phase composite composed of a matrix and pores, as shown in Fig. 9(b). It was difficult to experimentally determine the elastic modulus of the icicles, so a step-by-step approach was used

here to construct a computational model. The Hansen model [20] was used to model the elastic modulus of dried and ice-containing ALWSCC composites in Eqs. (6) and (7), respectively.

$$E_{dc} = E_m \times \frac{(1-V_p)E_m + (1+V_p)E_p}{(1+V_p)E_m + (1-V_p)E_p} \qquad (6)$$

$$E_c = E_m \times \frac{(1-V_i)E_m + (1+V_i)E_i'}{(1+V_i)E_m + (1-V_i)E_i'} \qquad (7)$$

where E_m, E_{dc}, E_p, E_c and E_i' are the elastic modulus of the matrix, dried ALWSCC, air, ALWSCC that contains ice and ice crystals at cryogenic temperature, respectively, and V_p and V_i are the volume fractions of air and ice crystals, respectively.

The experimental data for E_c and E_{dc} at 20% V_i are shown in Table 3. The elastic modulus of the matrix and ice crystals were obtained separately by inversion. The elastic modulus of ice crystals increases with decreasing temperature, as shown in Fig. 10.

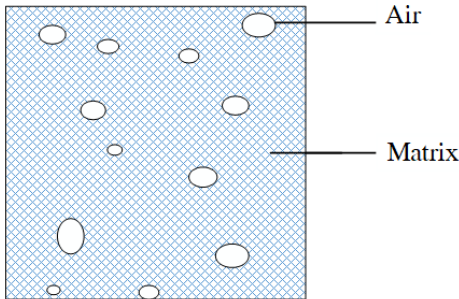(a) Composite model of ALWSCC that contains ice

(b) Composite model of dried ALWSCC
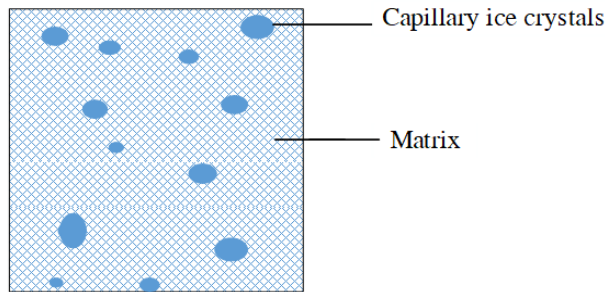
Fig. 9. Schematic diagram of the inclusion model of representative concrete elements.

The comparison of the elastic moduli of icicles and ice crystals is shown in Table 4. At the same temperature, the elastic modulus of ice crystals was much higher than that of icicles, exhibiting a large size effect. The size effect was relatively stable in the temperature interval of -5°C to -15°C, with a mean value of 16.41 and a variance of 0.7047 for E_i'/E_i. The reasons could be explained as follows: the elastic modulus of the icicle was determined under unconfined lateral compression, while that of the ice crystals was determined by parametric inversion, which reflected the mechanical response in a multidirectional constrained state. Therefore, E_i' could also be called the effective elastic modulus.
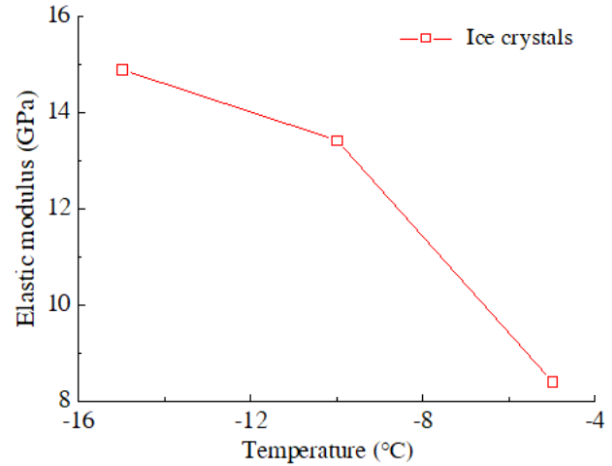

Fig. 10. Variation in the elastic modulus of ice crystals and icicles with temperature.

Table.3. Elastic modulus of ALWSCC, dry matrix and ice crystals at different cryogenic temperatures.

Group	-5 ℃	-10 ℃	-15 ℃
E_c (GPa)	23.96	26.15	27.33
E_{dc} (GPa)	20.02	20.38	21.03
E_m (GPa)	30.03	30.57	31.55
E_i (GPa）	8.42	13.43	14.90

Table 4. Comparison of elastic moduli for ice crystals and icicles.

Group	E_i' (MPa)	E_i (MPa)	E_i'/E_i	average of E_i'/E_i	Variance of E_i'/E_i
-5 ℃	8420	496.28	16.97		
-10 ℃	13430	788.70	17.03	16.41	0.7047
-15 ℃	14900	979.20	15.22		

5. Conclusions

To analyse the mechanism for the effects of ice crystals on the mechanical properties of lightweight aggregate concrete, mechanical tests were conducted on icicles and ALWSCC specimens in a cryogenic environment. The changes in the elastic modulus of ice crystals was analysed by micromechanical methods, and the main conclusions are as follows:

(1) The density of the icicles stabilized after 3 d in a cryogenic environment. The density and strength of icicles increased as the freezing temperature decreased over the range from -5°C to -15°C. There was a good linear relationship between the elastic modulus and density of the icicles. During compression, the icicles exhibited typical brittle material properties, and shear failure was the dominant mode.

(2) The compressive strength of the ALWSCC specimens increased as the volume fraction of ice crystals increased, and the strengthening effect of the ice crystals on the ALWSCC specimens gradually decreased after exceeding 16.5%. Both the compressive strength and elastic modulus of the ALWSCC specimens increased with decreasing cryogenic temperature, and the compressive strength of the ALWSCC specimens that contained ice crystals was more sensitive than the dried ALWSCC specimens to the cryogenic temperature.

(3) The elastic modulus of the ice crystals gradually increased with decreasing temperature according to a micromechanical analysis. The elastic modulus was much higher for the ice crystals than the icicles at the same temperature, which showed a huge size effect. The size effect was relatively stable in the temperature range from -5℃ to -15℃, and the mean value of E_i'/E_i was 16.41.

Since some cryogenic regions experience a large variation in temperature, and the buildings constructed of lightweight aggregate concrete materials undergo freeze-thaw cycling. The effects of ice crystals on the freeze-thaw damage of lightweight aggregate concrete is a future research direction.

References

1. Solonenko, I., "The use of cement concrete pavements for roads, depending on climatic conditions". *Technical Journal*, 13(3), 2019, pp. 235-240.
2. Wang, S. R., Wu, X. G., Yang, J. H., Zhao, J. Q., Kong, F. L., "Mechanical behavior of lightweight concrete structures subjected to 3D coupled static–dynamic loads". *Acta Mechanica*, 231(11), 2020, pp. 4497-4511.
3. Gintautas, S., Asta, K., Harald, J., Ina, P., "Effect of calcium nitrate on the properties of portland-limestone cement-based concrete cured at low temperature". *Materials*, 14(7), 2021, pp. 14071611.
4. Jian, X., Li, X. M., Wu, H. H., "Experimental study on the axial-compression performance of concrete at cryogenic temperatures". *Construction and Building Materials*, 72, 2014, pp. 380-388.
5. MacLean, T. J., Lloyd, A., "Compressive stress-strain response of concrete exposed to low temperatures". *Journal of cold regions engineering*, 33(4), 2019, pp. 04019014.
6. Chatterji, S., "Aspects of the freezing process in a porous material–water system: Part 1. Freezing and the properties of water and ice". *Cement and Concrete Research*, 29(4), 1999, pp. 627-630.
7. Masad, N., Dan, Z., Kim, S. M., Grasley, Z., "Meso-scale model for simulations of concrete subjected to cryogenic temperatures". *Materials and Structures*, 49(6), 2016, pp. 2141-2159.
8. Jiang, Z., Deng, Z., Zhu, X., Li, W., "Increased strength and related mechanisms for mortars at cryogenic temperatures". *Cryogenics*, 94, 2018, pp. 5-13.
9. Wang, Y., Damien, D., Xi, Y. P., "Micro- and meso-mechanical modeling of effect of freezing on modulus of elasticity of concrete". *Engineering Fracture Mechanics*, 200, 2018, pp. 401-417.
10. Jiang, Z. W., He, B., Zhu, X. P., Ren, Q., Zhang, Y., "State-of-the-art review on properties evolution and deterioration mechanism of concrete at cryogenic temperature". *Construction and Building Materials*, 257(10), 2020, pp. 119456.
11. Masad, N., Zollinger, D., Kim, S. M., Grasley, Z., "Meso-scale model for simulations of concrete subjected to cryogenic temperatures". *Materials and Structures*, 49(6), 2016, pp. 2141-2159.
12. Zhang, X. G., Kuang, X. M., Wamg, F., Wang, S. R., "Strength indices and conversion relations for basalt fiber-reinforced recycled aggregate concrete". *Dyna*, 94(1), 2019, pp. 82-87.
13. Zhang, X. G., Wang, S. R., Gao, X., He, Y. S., "Seismic behavior analysis of recycled aggregate concrete-filled steel tube column". *Journal of Engineering Science and Technology Review*, 12(4), 2019, pp. 129-135.
14. Kogbara, R. B., Iyengar, S. R., Grasley, Z. C., Rahman, S., Masad, E. A., Zollinger, D. G., "Relating damage evolution of concrete cooled to cryogenic temperatures to permeability". *Cryogenics*, 64, 2014, pp. 21-28.
15. Liu, X. M., Zhang, M. H., Chia, K, S., Yan, J. B., Liew, J. Y. R., "Mechanical properties of ultra-lightweight cement composite at low temperatures of 0 to -60 degrees C". *Cement and Concrete Composites*, 73, 2016, pp. 289-298.
16. Hansen, T. C., "Thermal and electrical conductively and modulus of elastici-ty of two-phasecomposite materials". *Rilem Ball*, 31, 1966, pp. 353-356.
17. Zhang, Y. X., Pan, J. W., Sun, X. J., Feng, J. J., Sheng, D. Q., Wang, H. Y., Zhou, X. J., He, Y. P., Diao, M. S., Zhan, Q. B., "Simulation of thermal stress and control measures for rock-filled concrete dam in high-altitude and cold regions". *Engineering Structures*, 230, 2021, pp. 111721.
18. Rostásy, F. S., Schneider, U., Wiedemann, G., "Behaviour of mortar and concrete at extremely low temperatures". *Cement and Concrete Research*, 9(3), 1979, pp. 365-376.
19. Jiang, Z. W., Deng, Z. L., Zhu, X. P., Li, W. T., "Increased strength and related mechanisms for mortars at cryogenic temperatures". *Cryogenics*, 94, 2018, pp. 5-13.
20. Gong, F., Wang, Y., Ueda, T., Zhang, D., "Modeling and mesoscale simulation of ice-strengthened mechanical properties of concrete at low temperatures". *Journal of Engineering Mechanics*, 143(6), 2017, pp. 04017022.
21. Xie, J., Yan, J. B., "Experimental studies and analysis on compressive strength of normal-weight concrete at low temperatures". *Structural Concrete*, 19(4), 2018, pp. 1235-1244.
22. Wu, X. G., Wang, S. R., Yang, J. H., Zhu, S., "Experimental study on mechanical performances of different fiber reinforced lightweight concretes". *Revista Romana de Materiale-Romanian Journal of Materials*, 49(3), 2019. pp. 434-442.